Silicon
https://doi.org/10.1007/s12633-021-01569-4

ORIGINAL PAPER

Effect of Chemical Treatment on Silicon Manganese: Its Morphological, Elemental and Spectral Properties and Its Usage in Concrete

Chin Mei Yun[1] · Muhammad Khusairy Bin Bakri[2] · Md Rezaur Rahman[2] · Kuok King Kuok[1] · Perry Law Nyuk Khui[2] · Durul Huda[3]

Received: 5 October 2021 / Accepted: 21 November 2021

Abstract
The effect of chemical treatment on silicon manganese slag and the effect of curing time on the compressive strength of completely replacement coarse aggregate silicon manganese concrete (SMC) relative to normal weight concrete (NWC) with gravel as coarse aggregate is the subject of this paper. Alkali and acidic base chemicals are used to alter the neat silicon manganese slag during chemical preparation. The mixture pattern proportions for Grade 30 and Grade 50, respectively, were used to create the concrete. Before the compressive strength tests, the samples were cast and cured for 7-, 14-, and 28-days. The properties of the silicon manganese slag and its concrete were studied using a scanning electron microscope (SEM), energy dispersive x-ray spectroscopy (EDS), and Fourier transform infrared spectroscopy (FTIR). The compressive strength of SMC30 and SMC50 obtained were 37.3 MPa and 51.1 MPa, respectively, on the 28-day. The alkaline treatment smoothest the matrix, while the acid treatment roughens the composition of the silicon manganese slag, according to SEM. The functional group demonstrated a major improvement in FTIR, while EDS revealed a high content of both silicon (Si) and manganese (Mn) elements. As a result, it can be observed that the power of SMC increases as the curing time increases for samples with complete replacement of normal aggregates using silicon slag.

Keywords Silicon · Manganese · Modification · Characterization · Applications · Concrete

1 Introduction

It has become more popular in the construction of many high-rise buildings due to the vast growth in every country worldwide, particularly in the big city, which emphasized the conservation and sustainability against the environment [1–6]. These high-rise buildings play an important role in housing the communities, while minimizing environmental impact [1–6]. The lightweight concrete structural, which uses either natural or artificial lightweight aggregates [7], is commonly used in these high-rise structures, which are made up of a combination of heavyweight and lightweight materials. Through lighter weight of construction materials used in massive self-weight structures, a low weight unit of lightweight structural concrete has been produced [1–6]. Many scarce natural lightweight materials, such as shale, limestone, and sand, may be conserved with the increment usage as construction materials, hence artificial light weight aggregates are source as alternative replacement [8–10]. However, it was top developed and emerging countries such as China, Russia, India, Korea, Japan, the United States, and Australia that contributed to technical understanding on the use of artificial aggregates. Malaysia is only a few years behind the rest of the world in terms of technological innovation [11, 12]. Despite the current environmental damage and aggregate source depletion problems, there is little

✉ Chin Mei Yun
mychin@swinburne.edu.my

✉ Muhammad Khusairy Bin Bakri
kucaigila@yahoo.com

✉ Md Rezaur Rahman
rmrezaur@unimas.my

[1] Faculty of Engineering, Computing and Science, Swinburne University of Technology Sarawak Campus, 93350 Kuching, Sarawak, Malaysia

[2] Faculty of Engineering, Universiti Malaysia Sarawak, Jalan Datuk Mohammad Musa, 94300 Kota Samarahan, Sarawak, Malaysia

[3] Department of Mechanical Engineering and Product Design Engineering, Swinburne University of Technology, Hawthorn, Victoria 3122, Australia

Published online: 07 January 2022

research on aggregate use and development as a substitute for natural lightweight by using artificial aggregates, especially in Malaysia [13].

Using the example of one of the most popular and effective byproducts in the world, bottom and fly ash as a combusted inorganic material, which is considered to be used as artificial lightweight aggregates from raw material due to its volume expansion stability [14–16]. However, greenhouse gases are highly created and extracted by thermal power plants where a significant amount of energy is required, which is expensive, as the production of artificial lightweight aggregates may require a sintering process at 900–1300 °C, which is typically combined with an inorganic material [17]. To address these issues, various studies have been performed using physical non-sintering coal ash processing processes, such as generating aggregates by mixing with binders [18–20].

Apart from blast furnace slag, which was traditionally used as a concrete admixture, most slags produced in the steel, iron, or metal industries have no applications due to their extraction process and technique [21]. However, owing to underdevelopment and a lack of research information on the usage of blast furnace slags in Malaysia, these slags are simply thrown away in the landfill as waste [22]. The lack of awareness and misinterpretation that most slags generated contain significant amounts of iron oxides (Fe-oxides), free-calcium oxide (free-CaO), and free-magnesium oxide (free-MgO) may explain the lack of information toward the application [23]. The majority of these free-CaO and -MgO can form during slow cooling, while the amorphous phase forms during rapid cooling, and the high-temperature molten slag has an amorphous structure until cooling [24–26]. Despite their Fe-based hydroxides, $Mg(OH)_2$, and $Ca(OH)_2$ forms, the majority of these compounds extend as they come into contact with water [27–29]. Furthermore, most steel slags produced had high thermal conductivity and net mass, making them unsuitable for use in normal-weight concrete. Slags are not used as by-products as fillers, binders, or aggregates for concrete in Malaysia, and have never been used as raw materials for any artificial lightweight aggregates. The Malaysian Standard (MS) and the Works Department (WD)do not have it completely registered and standardized. Furthermore, the Department of Environment (DOE) classifies it as a schedule waste. As a result, extensive research is needed to determine the most suitable use of slags as a building material.

A nonferrous metal, silicon manganese (SiMn) slag, is produced during the smelting process. It contains a lot of Si-based oxide and a little Fe-based oxide. Frias et al. [30] identified a fine SiMn slag powder suitable for use as aggregate in concrete, which improves volumetric and thermal stability when used as a cement admixture [31, 32]. The molten SiMn slag induces water evaporation when it comes into contact with water due to its high thermal temperature, which created small pores on the inner layer of the slag and large pores on the outer slag layer as the cooling process progressed. Since the pore formation could intimidate an important lightweight aggregates resource, it has a lot of potential for commercialization in construction and building materials, particularly in Malaysia.

The three most popular cooling methods are (i) air cooling, (ii) water cooling (by quenching), and (iii) compound quenching (by oil, chemical aqueous solution, etc.). Furthermore, slow cooling by air-cooled by leaving the slag in an open storage until it cooled for a certain time, if sprinkling occurred, either through water, etc., can have a variety of effects on the slag's consistency, with dust, restricted open storage, and leachate generation all contributing to the issues [33]. Furthermore, most molten SiMn slag in Malaysia are condensed, solidified as big rocks, and deposited as waste in landfills, while it needed to be compressed to be used as coarse aggregate. This results in a rise in waste in the landfill's small capacity.

In this paper, the potentials of SiMn slag aggregates are reported, in which SiMn slag aggregates were studied using alkali, acid, and heat treatment in this analysis. To describe and analyses the effect of chemical and heat alteration on SiMn slag, limestone, Ordinary Portland Cement (OPC), and Silicon Manganese Concrete, scanning electron microscopy (SEM), energy dispersive x-ray spectroscopy (EDX/EDS), and Fourier transform infrared spectroscopy (FTIR) are used (SMC). A fundamental research wasalso carried out to compare and measure the usability of SiMn Slag Manganese Concrete (SMC) as standard concrete aggregates with OPC. The concrete's compressive strength was compared to that of Normal Weight Concrete (NWC), and the compression strength properties of both were investigated and documented.

2 Methodology

2.1 Materials

Silicon manganese slag (SiMn slag) was obtained from OM Materials Sdn. Bhd., Bintulu, Sarawak, Malaysia. Ordinary Portland cement (OPC) were obtained from Cahaya Mata Sarawak (CMS) Berhad. Kuching, Sarawak, Malaysia. Crushed aggregates as coarse aggregates for NWC and river sand as fine aggregates for both NWC and SMC were obtained locally from Sarawak. Plasticizing REAL FLOW 671 admixuture cement was supplied by Real Point Sdn. Bhd, Selangor Malaysia. For chemical treatment, sodium hydroxide, NaOH (alkaline) (CAS 1310-73-2), hydrochloric acid, HCl (acidic) (CAS 7647-01-0), sulfuric acid, H_2SO_4 (acidic acid) (CAS 7664-93-9) were used. These inorganic

chemicals were supplied by Fisher Scientific International, Inc. from United States. The caustic soda of NaOH obtained is industrially produced through electrolytic chloralkaline process. It is dissolves in water to form a colorless solution. HCl obtained is in aqueous form captured from hydrogen chloride gas. It is soluble in water and alcohol, clear and colorless liquid with strong pungent smell, which act as reagent for samples. H_2SO_4 is formed naturally oxidation of sulfide mineral. It also commercially produced when sulfur trioxide is dissolved in water.

2.2 Silicon Manganese Slag Chemical Treatment

The obtained silicon manganese, SiMn slag was divided into 4 categories: Neat-SiMn, NaOH-SiMn, HCl-SiMn, H_2SO_4-SiMn. For chemical treatment, solution was created by mixing 5 wt% of caustic soda of NaOH with 95 wt% of distilled water to prepare NaOH solution, 5 wt% aqueous of HCl with 95 wt% of distilled water to prepare HCl solution, 5 wt% aqueous of H_2SO_4 with 95 wt% of distilled water to prepare H_2SO_4 solution. The solid SiMn was crunch into 10 mm size and soaked in each of the chemical solution to create modified NaOH-SiMn, HCl-SiMn, and H_2SO_4-SiMn for 15 min before filtered and dry for heat treatment in an open-ventilated drying oven for 30 min under temperature of 90 °C.

2.3 Concrete Mixture Proportions

The mixture proportions design is shown in Table 1. It was designed to achieve a concrete compressive strength of Grade 30 MPa (which is labeled as NWC30 and SMC30) and Grade 50 MPa (which is labeled as NWC50 and SMC50), respectively. Silicon manganese slag was used as coarse aggregates for SMC. Meanwhile, for NWC, gravel was used as the coarse aggregates. Both samples, NWC and SMC used 20 mm size coarse aggregates. For the fine aggregates, river sand was used. The admixture used has an admixture of high-range water-reducing and set-retarding for concrete, which complied with Type B, D and G of ASTM C494–19 [34] and BS 5075–1:1982 [35]. The specifications and the amount were shown in Table 1 for each concrete type.

Table 1 The Mixture Proportions for normal weight concrete (NWC) and silicon manganese concrete (SMC)

Mix Proportions by Weight (kg/m^3)	NWC30	NWC50	SMC30	SMC50
Cement	360	500	360	500
Fine Aggregate	730	710	730	710
Coarse Aggregate	1100	1040	1100	1040
Water	166	168	166	168
Admixture (ml)	2880 ml	5500 ml	2880 ml	5500 ml
Water to binder ratio	0.46	0.34	0.46	0.34

2.4 Concrete Preparation

For each batch of concrete, nine samples of concrete cubes were prepared. The samples were cast, cured and tested on the 7-day, 14-day, and 28-day, respectively. During the cast for NWC30 and NWC50, natural river sand and crushed aggregates was used for fine and coarse aggregate, respectively. While for SMC30 and SMC50, natural sand and silicon manganese slag was used for fine and coarse aggregates, respectively. The samples were mixed using concrete mixing drum according to mixture proportions shown in Table 1. Water with respect to water to binder ratio shown in Table 1 was added into the concrete mixture, and the concrete were mixed thoroughly for 15 min. The concrete mixture was then placed into the concrete steel cube molds of 150 mm X 150 mm X 150 mm with 3 equal layers of compaction applied. Compaction was carried out using vibration table to remove the entrapped air and to avoid segregation of particles. Subsequently, the concrete mixture in the steel cube molds were left to dry in the lab for 24 h before demolding were carried out. The samples were then placed in water tank filled with water, which cured up to 7 days, 14 days, and 28 days prior to compressive test. The procedures of casting and curing is in accordance the IS 10262:2019 standard [36].

2.5 Characterization and Testing

2.5.1 SEM and EDX/EDS Analysis

ASTM E2015–04 [37], ASTM E2142–08 [38], and ASTM C1723–16 [39] standards were used to perform scanning electron microscopy (SEM) with energy dispersive x-ray spectroscopy (EDX/EDS). A magnification of 500x was used to examine a variety of SiMn slag, granite, and ordinary Portland cement samples, as well as their concrete. Furthermore, EDX/EDS was performed in accordance with ASTM E1508–12 [40]. Three points were chosen at random from the neat and modified SiMn slag, limestone, Portland cement, and concrete samples. The elemental composition percentages analysis was automated by the program. The EDX/EDS was replicated several times for each study, and the most common findings were carefully selected. For the SEM and EDX/EDS, A Hitachi TM4000Plus Tabletop Microscope with a Quantax75™ Series Energy Dispersive X-Ray Spectrometer (Hitachi Ltd., Tokyo, Japan) was used to analyses the neat and modified SiMn, limestone, ordinary Portland cement, and silicon manganese concrete (SMC) samples to investigate its composition, size and surface structure.

2.5.2 FTIR Analysis

A Fourier-transform infrared spectroscopy (IRAffinity^{-1}, Shimadzu Corporation, Kyoto, Japan) was used for the FTIR analysis of the neat and modified SiMn slag, limestone, ordinary Portland cement, and SiMn slag aggregate concrete (SMC) samples for comparison. Fourier-transform infrared spectroscopy was conducted according to the ASTM E168–16 [41] and ASTM E1252–98 [42] standards for qualitative and quantitative analysis. The spectrum scanning was conducted in the wavenumber range of 4000 cm^{-1} to 400 cm^{-1} for each sample. Fourier-transform infrared spectroscopy utilized the infrared spectrum transmittance and absorption of the samples to develop a unique molecular fingerprint spectrum. The test was repeated numerous times for each sample, and the most representative results were selected.

2.5.3 Compressive Test

On the testing day, the concrete samples were removed from the water tank and the compressive strength test was conducted in accordance with BS EN 196–1:2016 [43] using the electrically operated U20CrEL Model of Motorized Hydraulic Compression Testing Machine. During the compressive test, load was applied gradually on top of the concrete samples at 2.4 ± 0.2 kN/s, until the samples failed. Results obtained from the same three concrete batch samples of on same testing days with respect to 7-, 14- and 28-days were averaged and reported.

3 Results and Discussions

3.1 Compressive Strength

Figure 1 shows the compressive strength of NWC and SMC with full replacements of gravels using silicon manganese slag at 7-, 14- and 28-days. For both NWC and SMC, the compressive strength increases with the curing duration. Although SMC samples had shown slightly lower compressive strength compared to NWC at all curing period, SMC30 and SMC50 achieved compressive strength of 37.3 MPa and 51.1 MPa at the 28-days, which passed Grade 30 and Grade 50 mixture design proportion standards. At the 7-days, SMC30 demonstrate 6.3% compressive strength reduction compared to NWC30 whilst SMC50 achieve 10% compressive strength lesser than NWC50. At the 14-days, SMC30 achieve comparable compressive strength with NWC30 while SMC50 demonstrate 16% compressive strength reduction compared to NWC50. While at the 28-days, SMC30 and NWC30 displayed comparable compressive strength. However, SMC50 shown 9.2% compressive strength reduction compared to NWC50.

It was observed that both NWC and SMC samples had surpassed the typical specified compressive strength for structural application of 30 MPa and 50 MPa. Ganesh et al. [44] found a similar result for Grade 30 concrete, where the complete substitution of coarse aggregates with silicon manganese slag reached 30.44 MPa at the 28-day with a slightly lower cement content of 330 kg/m^3 and a slightly lower cement content of 330 kg/m^3.

3.2 Morphological Analysis

SEM photographs of limestone, ordinary Portland cement, and silicon manganese slag aggregate concrete are seen in

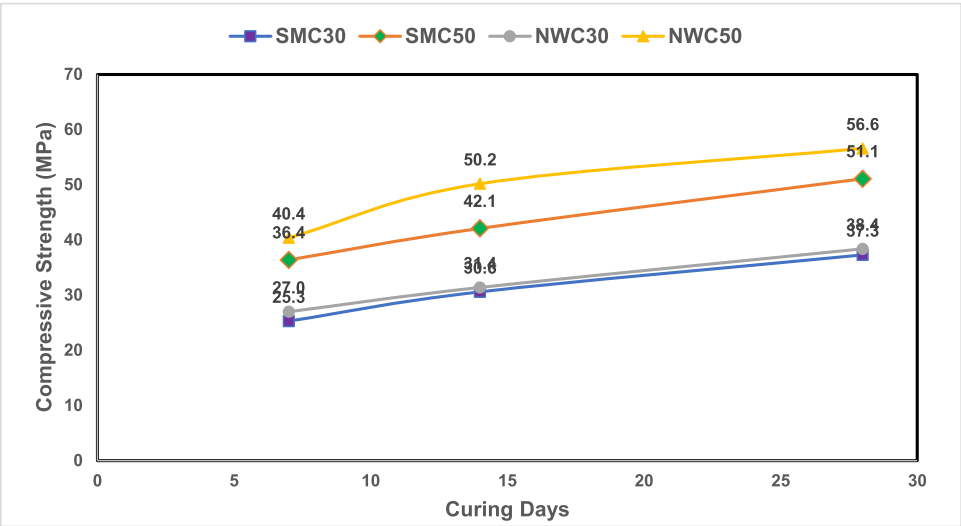

Fig. 1 The compressive strength of normal weight concrete (NWC) and silicon manganese concrete (SMC)

Fig. 2 (a), (b), and (c) at 500x magnification (SMC). Figure 2 (a) depicts a limestone sample aggregate that was used in architecture, housing, paving, and road materials in Sarawak, Malaysia. According to the samples, the limestone is brittle mosaic in surface structures of inconsistent grain size, with some having small soft bit structures that vary in form and grove [45–48]. Many researchers [49] have stated that the brittle and inconsistently sized, shapes, groove surface structures, and poor hydration of limestone can cause weak adhesion at certain parts of the concrete and composites, particularly when bonded with polymer, bitumen, or cement. Initial cracks may occur before or after the limestone has been bonded, particularly when the materials are loaded [49]. When a load is added to the components, this results in a random breaking point at a certain region of the threshold [49].

The ordinary Portland cement without admixture is seen in Fig. 2(b). The hydration process was irregular, as there was a combination of un-hydrated and hydrated cement in some areas, resulting in a small size crack on the cement surface [50]. In contrast, Fig. 2(c) depicts a slight crack between the silicon manganese slag and ordinary Portland cement used by SMC. The smooth surface of silicon manganese slag slipped, transferred, or moved due to the load added to it during the compressive strength test, which was also a typical failure in many forms of concrete [50–52]. It is also worth noting that for SMC, the interaction between sand and other materials is correctly combined, resulting in better samples.

Figure 3(a), (b), (c), and (d) reveal images of Neat-SiMn, NaOH-SiMn, HCl-SiMn, and H2SO4-SiMn slag at 500x magnification. The alkaline treatment results in a smoother surface with less grain, as seen in Fig. 3(b), while the acidic treatment results in porosity on the surface of the silicon manganese slag, as seen in Fig. 3(c) and (d). It was also discovered that different chemical compositions and concentrations on the surface of the silicon manganese slag produce different reactions. The acid concentration and composition in Fig. 3(d) appear to produce a special needle fascinated shape, resulting in a rougher and more readily absorbent surface [53]. When comparing Fig. 3(c) and (d), it can be shown that the acidic concentration and composition appear to eliminate unwanted weak structures, resulting in a small amount of porous structure on the surface [53].

3.3 EDX/EDS Analysis

Tables 1, 2 and 3 shows the EDS/EDX elemental analyses for limestone, ordinary Portland cement, and silicon manganese concrete (SMC). Figures 4, 5, and 6 depicted the graph continuum of Tables 2, 3 and 4 correlation results, respectively. Carbon (C), oxygen (O), calcium (Ca), natrium (Na), and chlorine (Cl) were found in the samples, according to Table 2. Table 3 shows the presence of carbon (C), calcium (Ca), oxygen (O), silicon (Si), potassium (K), natrium (Na),

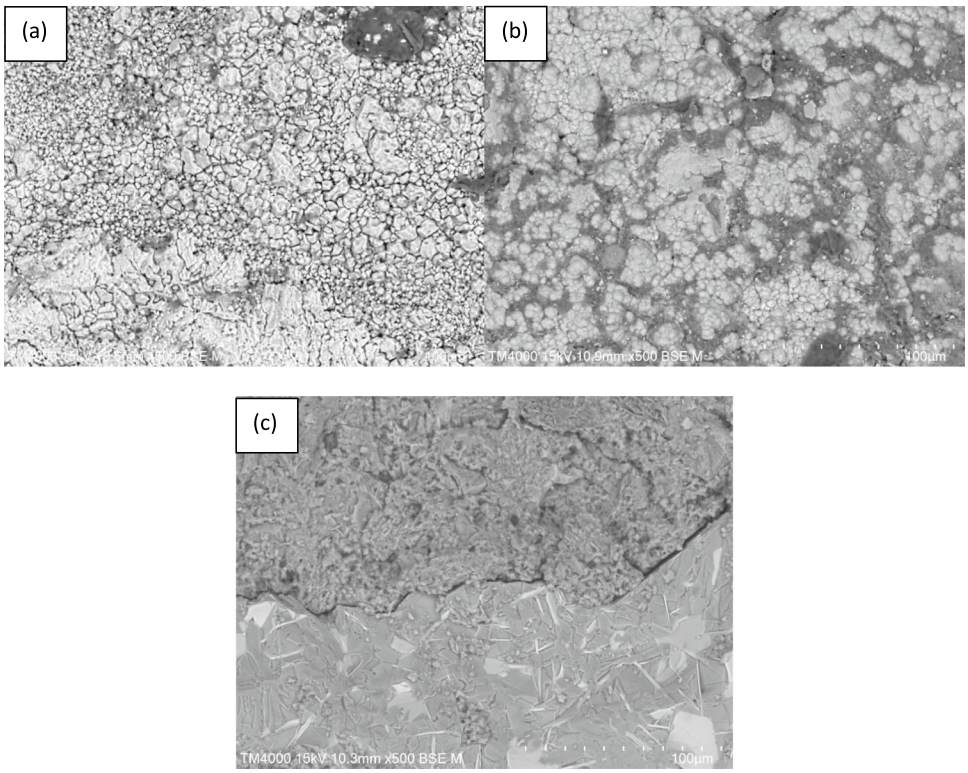

Fig. 2 The SEM images at 500x magnification for (**a**) limestone, (**b**) ordinary Portland cement (OPC), and (**c**) silicon manganese concrete (SMC)

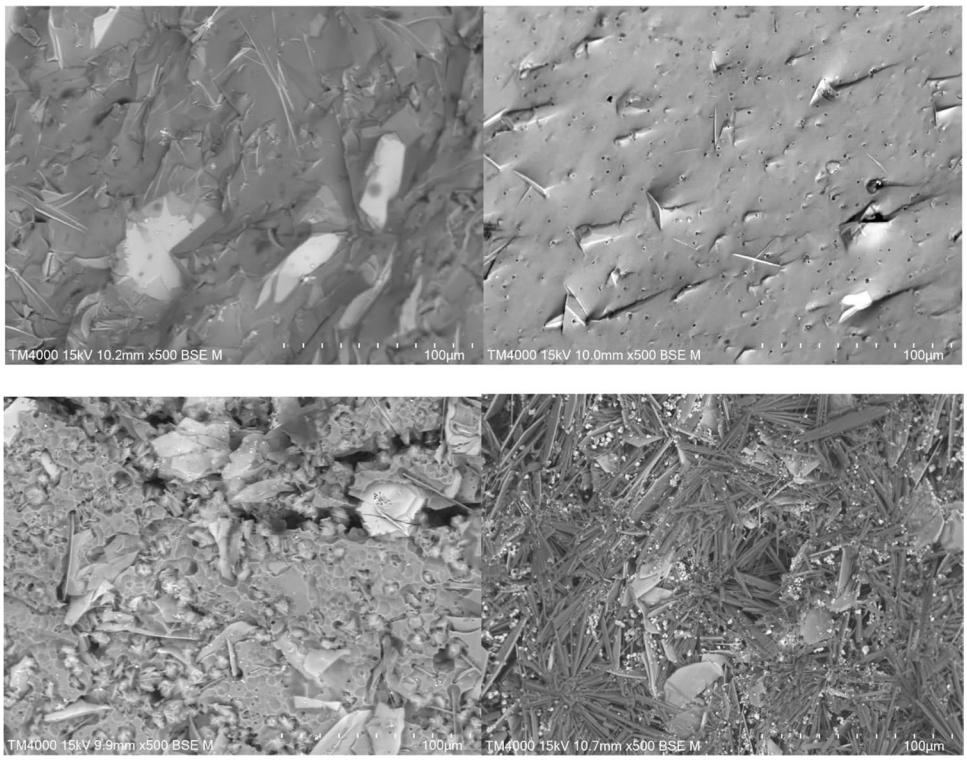

Fig. 3 The SEM images at 500x magnification for (**a**) Neat silicon manganese (Neat-SiMn), (**b**) Treated sodium hydorixe silicon manganese (NaOH-SiMn), (**c**) Treated hydrochloric acid silicon manganese (HCl-SiMn), and (**d**) Treated sulfuric acid silicon manganese (H_2SO_4-SiMn)

Table 2 EDS element composition for limestone

Element	Atomic No.	Mass Normal (%)	Atom (%)	Absolute Error (%) (1 sigma)	Relative Error (%) (1 sigma)
O	8	47.05	54.89	6.78	12.52
Ca	20	33.59	15.64	1.18	3.05
C	6	18.62	28.94	2.83	13.22
Na	11	0.50	0.41	0.07	12.07
Cl	17	0.24	0.12	0.04	14.15
Total		100	100		

Table 3 EDS element composition for ordinary Portland cement (OPS)

Element	Atomic No.	Mass Normal (%)	Atom (%)	Absolute Error (%) (1 sigma)	Relative Error (%) (1 sigma)
O	8	41.72	48.86	5.72	12.82
Ca	20	32.51	15.20	1.07	3.06
C	6	21.15	33.00	3.01	13.31
Si	14	1.97	1.31	0.12	5.57
K	19	1.01	0.48	0.06	5.91
Na	11	0.79	0.64	0.09	10.19
Cl	17	0.51	0.27	0.05	8.69
Al	13	0.34	0.24	0.05	12.74
Total		100	100		

chlorine (Cl), and aluminium (Al) throughout the samples. Figures 4 and 5 and Tables 2 and 3 indicate that oxygen has the largest mass percentage, followed by calcium and carbon, while other elements have low mass percentages. This shows that limestone contained mostly $CaCO_3$, CaO, Na_2O, and slight amount of NaCl [54]. While ordinary Portland cement

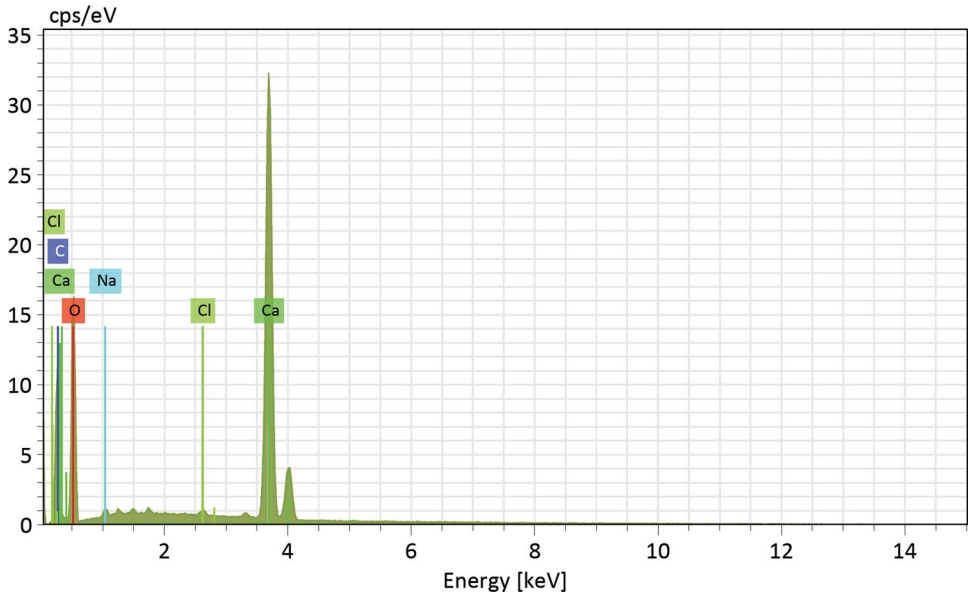

Fig. 4 EDS spectrum graph of limestone

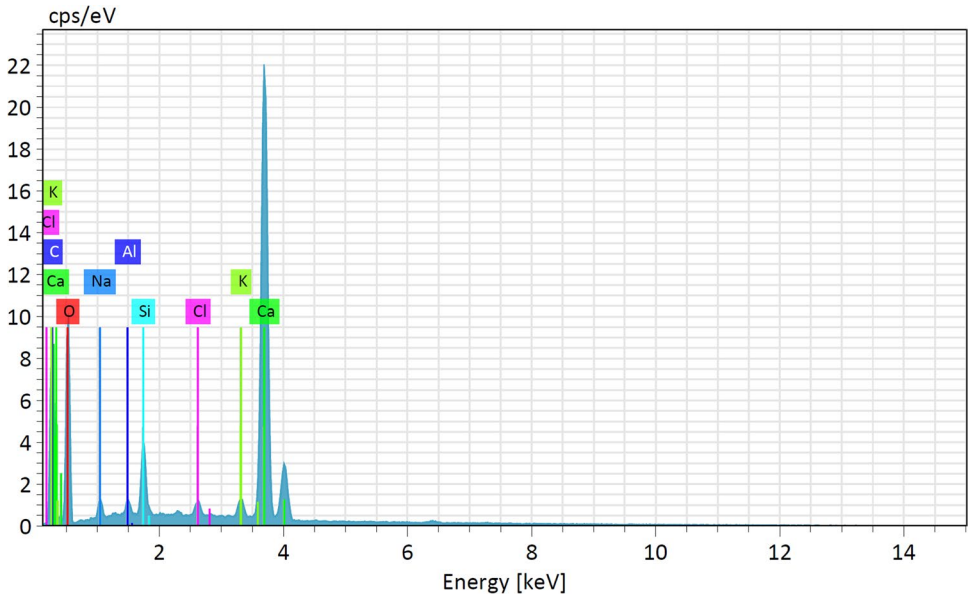

Fig. 5 EDS spectrum graph of ordinary Portland cement (OPS)

contained mostly $CaCO_3$, CaO, SiO_2, Al_2O_3, Na_2O, K_2O, and slight amount of NaCl [55–57]. The present of $CaCO_3$ and CaO helps strengthen and increase the durability of the limestone and ordinary Portland cement, which also accelerate the effect of hydration reactivity rate [58]. However, the present of slight NaCl may promote corrosion towards steel in concrete, which make it weaker in long period [59, 60].

In silicon manganese concrete, as shown in Table 4, the present element in the samples were calcium (Ca), oxygen (O), silicon (Si), carbon (C), aluminium (Al), manganese (Mn), barium (Ba), magnesium, (Mg), natrium (Na), and potassium (K). From Fig. 6 and Table 4, it showed that oxygen had the highest content mass percentage, followed by calcium and silicon, while the other elements mass percentage remain low. This shows that silicon manganese concrete contained mostly $CaCO_3$, CaO, Na_2O, SiO_2, Al_2O_3, Na_2O, K_2O, BaO, $BaCO_3$, MgO, SiMn, MnO [4, 32]. The present of $CaCO_3$ and CaO helps strengthen concrete, and accelerate the effect of hydration rate, while BaO, and $BaCO_3$ increase the dense of the concrete [32, 58]. However, the absence of NaCl, especially chlorine, reduced corrosion effects towards steel in concrete, which could retain its strength in long period [4, 61, 62].

The EDS/EDX elemental analysis for Neat-SiMn, NaOH-SiMn, HCl-SiMn and H_2SO_4-SiMn slag are shown in Tables 5, 6, 7, and 8. While Figs. 7, 8, 9 and 10 showed the

graph spectrum correlation with data in Tables 5, 6, 7, and 8, respectively. Based on Tables 5, 6, 7 and 8, similar present element in all the samples were calcium (Ca), oxygen (O), silicon (Si), carbon (C), potassium (K), barium (Ba), and aluminium (Al). It is also noted that in the Neat-SiMn, NaOH-SiMn, and HCl-SiMn, there is a present of manganese (Mn), magnesium (Mg), and natrium (Na), even though it is not present in H_2SO_4-SiMn. NaOH treatment cause the present of nitrogen (N) in NaOH-SiMn, while HCl cause the present of chlorine (Cl) and lead (Pb), and H_2SO_4-SiMn

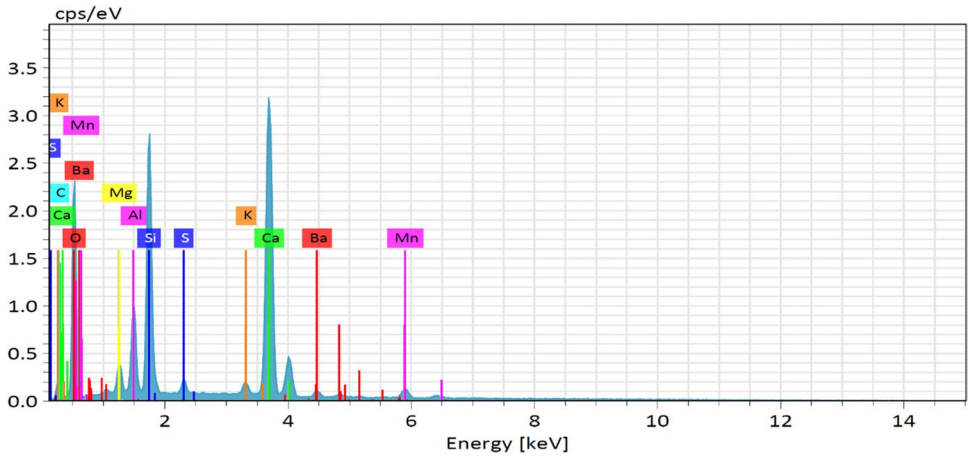

Fig. 6 EDS spectrum graph of silicon manganese cement (SMC)

Table 4 EDS element composition for silicon manganese cement (SMC)

Element	Atomic No.	Mass Normal (%)	Atom (%)	Absolute Error (%) (1 sigma)	Relative Error (%) (1 sigma)
O	8	46.33	63.38	4.29	12.67
Ca	20	29.35	16.03	0.67	3.12
Si	14	10.63	8.28	0.35	4.53
C	6	3.65	6.60	0.58	22.04
Al	13	3.36	2.73	0.14	5.85
Mn	25	2.93	1.17	0.10	4.85
Ba	56	1.75	0.28	0.08	5.89
Mg	12	1.07	0.97	0.07	9.18
K	19	0.70	0.39	0.05	8.91
Na	11	0.25	0.17	0.03	19.09
Total		100	100		

Table 5 EDS element composition for neat silicon manganese (Neat-SiMn)

Element	Atomic No.	Mass Normal (%)	Atom (%)	Absolute Error (%) (1 sigma)	Relative Error (%) (1 sigma)
O	8	44.63	55.73	6.36	12.18
Si	14	13.18	9.37	0.67	4.36
C	6	11.70	19.47	2.25	16.40
Ca	20	10.81	5.39	0.41	3.25
Al	13	6.77	5.01	0.40	5.04
Ba	56	5.18	0.75	0.22	3.63
Mn	25	4.03	1.47	0.18	3.91
Mg	12	2.34	1.92	0.18	6.52
K	19	0.82	0.42	0.06	6.48
Na	11	0.53	0.46	0.07	11.80
Total		100	100		

Table 6 EDS element composition for treated sodium hydroxide silicon manganese (NaOH-SiMn)

Element	Atomic No.	Mass Normal (%)	Atom (%)	Absolute Error (%) (1 sigma)	Relative Error (%) (1 sigma)
O	8	47.05	57.21	7.26	12.07
Si	14	13.51	9.36	0.75	4.34
C	6	10.13	16.41	2.17	16.77
Ca	20	10.09	4.90	0.42	3.25
Al	13	5.99	4.32	0.39	5.06
Mn	25	4.15	1.47	0.20	3.83
Ba	56	2.81	0.40	0.15	4.14
Mg	12	2.49	1.99	0.20	6.36
N	7	1.93	2.68	0.68	27.66
Na	11	0.99	0.84	0.11	9.09
K	19	0.87	0.43	0.07	6.06
Total		100	100		

Table 7 EDS element composition for treated hydrochloric acid silicon manganese (HCl-SiMn)

Element	Atomic No.	Mass Normal (%)	Atom (%)	Absolute Error (%) (1 sigma)	Relative Error (%) (1 sigma)
O	8	42.09	58.62	4.13	12.36
Si	14	13.39	10.62	0.47	4.44
Ca	20	11.27	6.27	0.30	3.35
Ba	56	10.90	1.77	0.29	3.36
Al	13	7.62	6.29	0.31	5.14
C	6	6.21	11.52	0.98	19.94
Mn	25	4.49	1.82	0.15	4.16
Mg	12	1.44	1.32	0.09	8.05
Cl	17	1.01	0.64	0.06	7.12
K	19	1.00	0.57	0.06	6.99
Na	11	0.58	0.56	0.06	13.25
Pb	82	0.00	0.00	0.00	1.51
Total		100	100		

Table 8 EDS element composition for treated sulfuric acid silicon manganese (H_2SO_4-SiMn)

Element	Atomic No.	Mass Normal (%)	Atom (%)	Absolute Error (%) (1 sigma)	Relative Error (%) (1 sigma)
O	8	56.54	71.56	7.53	11.96
Ca	20	14.88	7.52	0.53	3.19
S	16	11.08	6.99	0.47	3.78
Ba	56	7.30	1.08	0.28	3.44
C	6	5.75	9.69	1.25	19.46
Si	14	2.19	1.58	0.13	5.43
Al	13	1.79	1.34	0.12	6.23
K	19	0.48	0.25	0.05	9.10
Total		100	100		

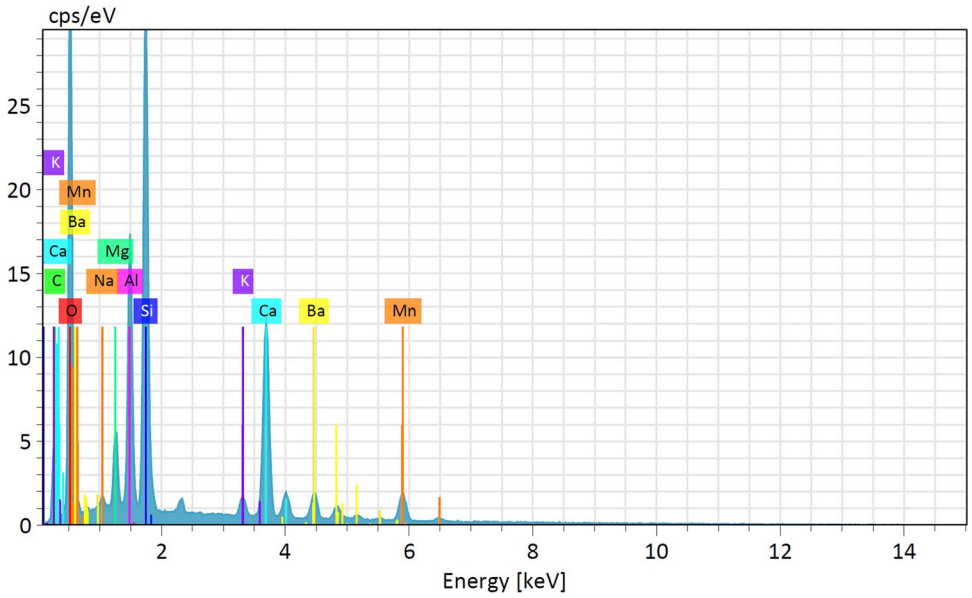

Fig. 7 EDS spectrum graph of neat silicon manganese (Neat-SiMn)

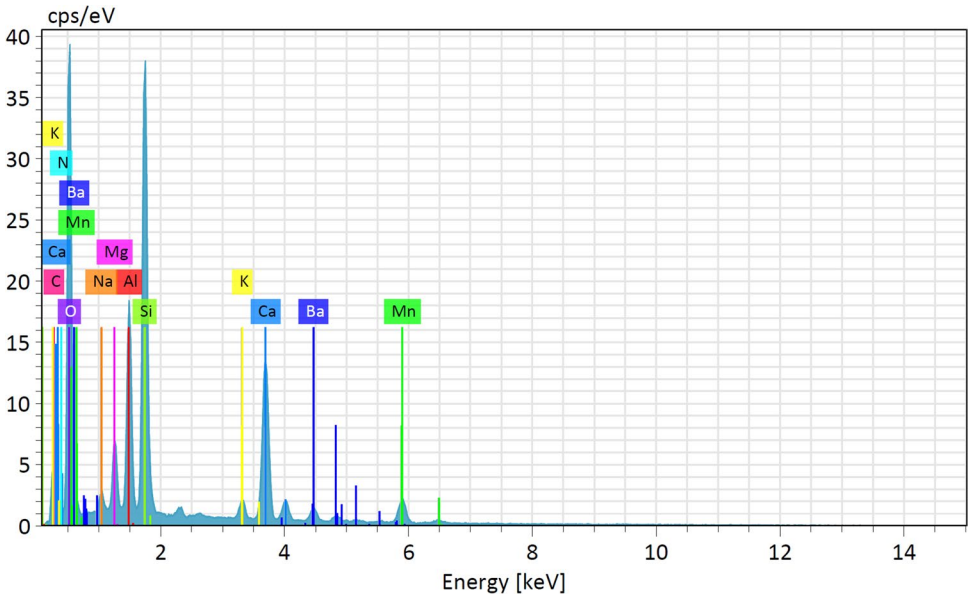

Fig. 8 EDS spectrum graph of treated sodium hydroxide silicon manganese (NaOH-SiMn)

cause the present of sulphur (S). From Figs. 7, 8, 9 and 10, and Tables 5, 6, 7 and 8, it showed that the highest content was oxygen mass percentage, while other elements mass percentage remain low. This shows that Neat-SiMn slag contained mostly $CaCO_3$, CaO, Na_2O, SiMn, Al_2O_3, BaO, $BaCO_3$, Na_2O, K_2O, SiO, SiO_2, and MgO [4, 32, 63–65]. While BaO, and $BaCO_3$ increase the density, $CaCO_3$ and CaO helps to strengthen by increasing the durability of silicon manganese slag, by accelerating the hydration reactivity rate [32, 58]. The present of SiO and SiO_2 created mixture of crystalline and amorphous structure, depending on the chemical reaction towards the chemical treatments, which was reflected in SEM result in Fig. 3.

From the analysis it is noted that there are few possible chemical reactions happened during the treatments. Equation (1) to (6) shows the possibilities of the chemical reactions.

$$Mn + 2HCl \rightarrow MnCl_2 + H_2 \quad (1)$$

$$Si + 2HCl \rightarrow SiCl_2 + H_2 \quad (2)$$

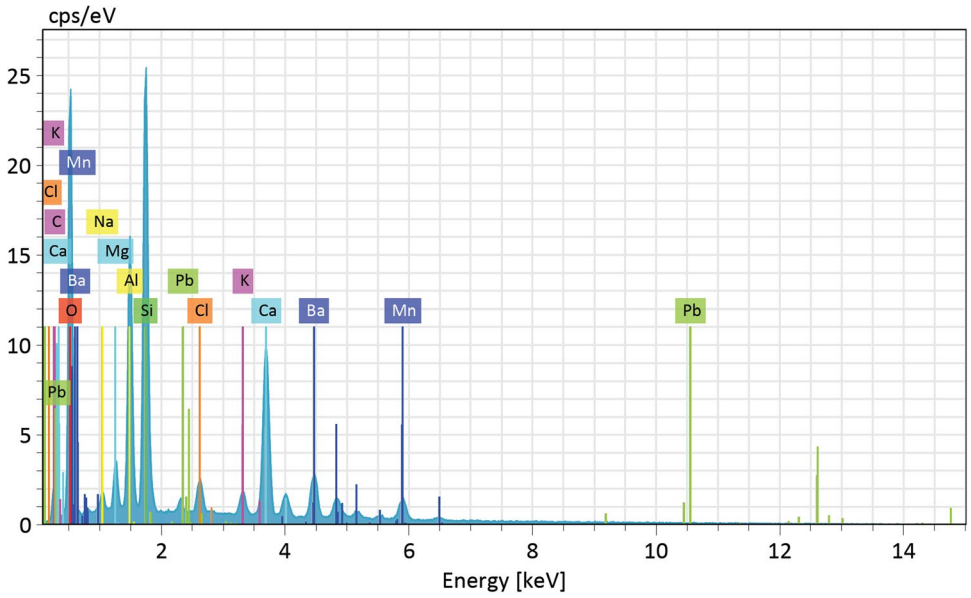

Fig. 9 EDS spectrum graph of treated hydrochloric acid silicon manganese (HCl-SiMn)

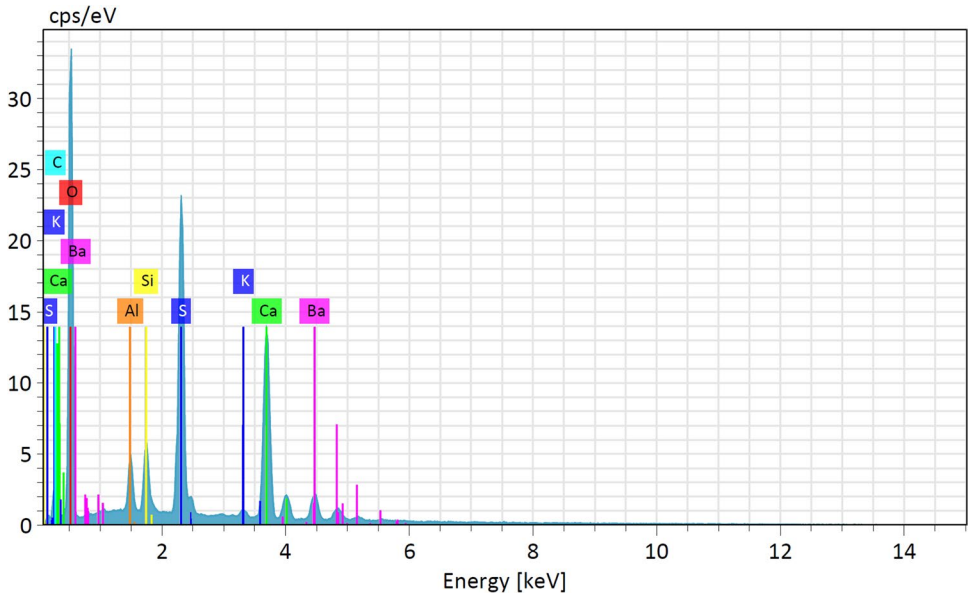

Fig. 10 EDS spectrum graph of treated sulfuric acid silicon manganese (H_2SO_4-SiMn)

$$Mn + H_2SO_4 \rightarrow MnSO_4 + H_2 \quad (3)$$

$$Si + H_2SO_4 \rightarrow SiO_2 + H_2O_2 \quad (4)$$

$$Mn + 2NaOH \rightarrow Mn(OH)_2 + 2Na \quad (5)$$

$$Si + 2NaOH + H_2O \rightarrow +Na_2SiO_3 + 2H_2 \quad (6)$$

3.4 FTIR Analysis

Figures 11, 12 and 13 shows the FTIR images for limestone, ordinary Portland cement and silicon manganese concrete. According to Fig. 13, the broad band intensity of 3500 cm^{-1}-3000 cm^{-1} designated to the water molecules, which is due to stretching of -OH and vibrations of H-0-H. The small sharp peaks in Fig. 11 at 3940 cm^{-1}, 3817 cm^{-1}, 3745 cm^{-1} and Fig. 12 at 3739 cm^{-1} was due to the free hydroxyl groups. This free hydroxyl group tend to react during hydraulic hydration process. The reaction caused the surface materials entrapped in cavities or void in the

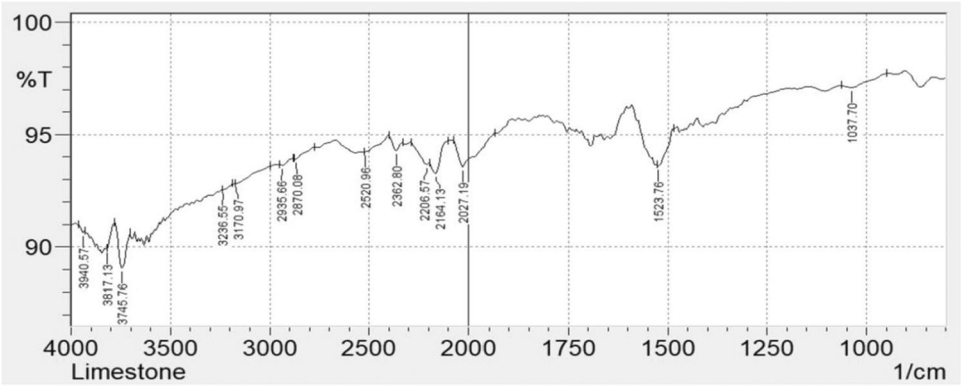

Fig. 11 FTIR spectrum graph for limestone

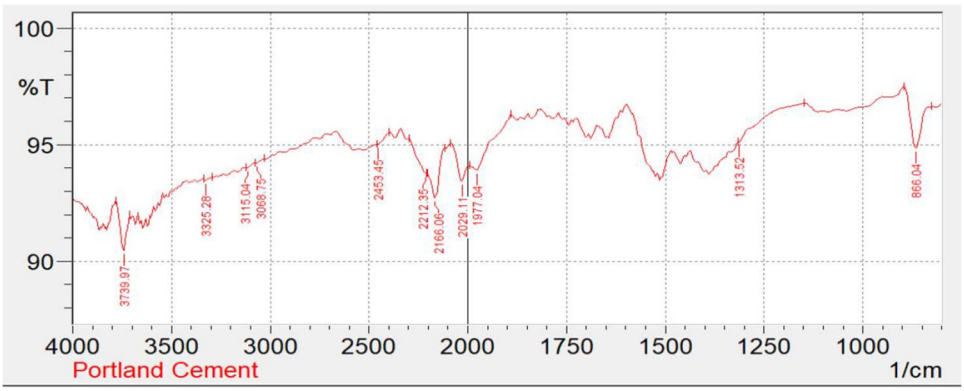

Fig. 12 FTIR spectrum graph for ordinary Portland cement (OPC)

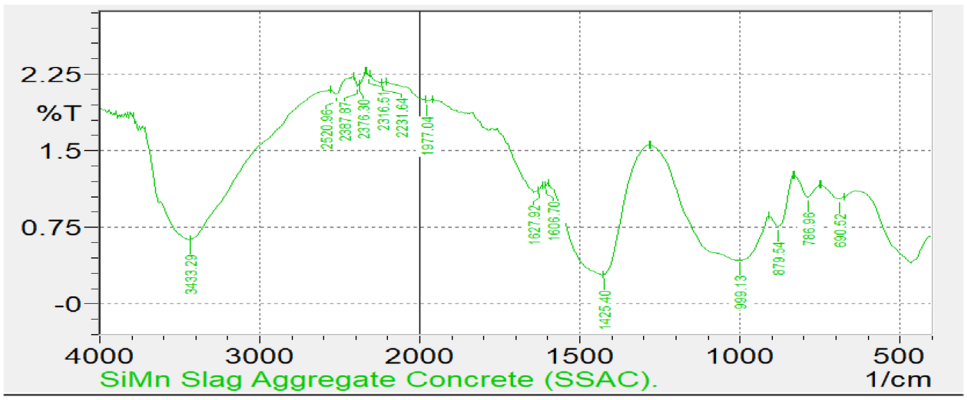

Fig. 13 FTIR spectrum graph for silicon manganese concrete (SMC)

polymeric framework. In Figs. 11, 12 and 13, few small sharp peaks spotted throughout the 2520 to 1037 cm^{-1}, 2453 to 866 cm^{-1}, 2520 to 690 cm^{-1}, absorption band was designated to the calcium in the form of calcite ($CaCO_3$) [66–68]. Whereas most CO_3^{2-} having asymmetric stretching, in-plane and out-of-plane bending [69]. In Fig. 13, at 1425 and 999 cm^{-1}, the peak was designated for asymmetric stretching and vibration of Si-O-Al and/or Si-O-Si, respectively [70, 71].

Figures 14, 15, 16 and 17 shows the FTIR images for Neat-SiMn, NaOH-SiMn, HCl-SiMn, and H_2SO_4-SiMn. It is noted that multiple peaks at 2000–2500 cm^{-1} was due to stretching vibration of Si-O and Si-Mn, which occurred in and out of phase for SiO for silicon manganese slag [70–72]. The alkaline treatment causes the peak almost diminished which shows the Si-Mn and Si-O structure were in plane, while acid caused the bending of Si-O and Si-Mn which at the end created rougher needle structure of

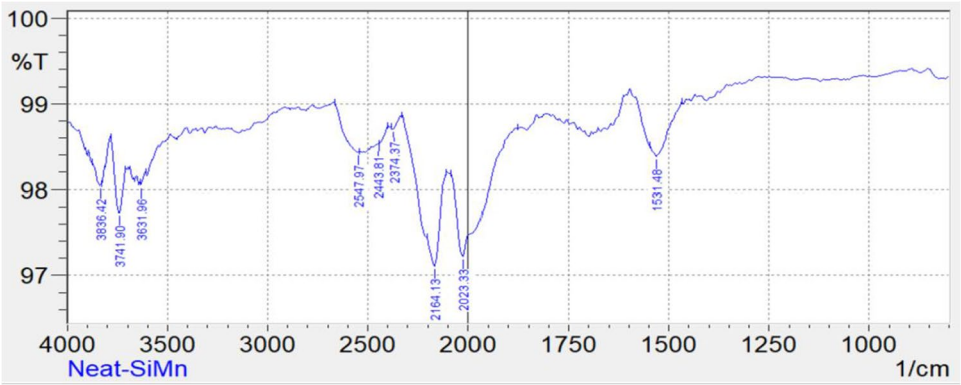

Fig. 14 FTIR spectrum graph for neat silicon manganese (Neat-SiMn)

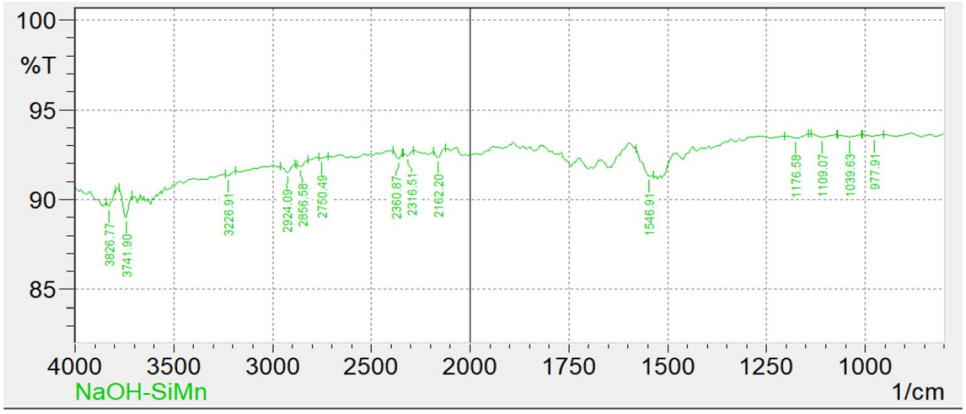

Fig. 15 FTIR spectrum graph for treated sodium hydroxide silicon manganese (NaOH-SiMn)

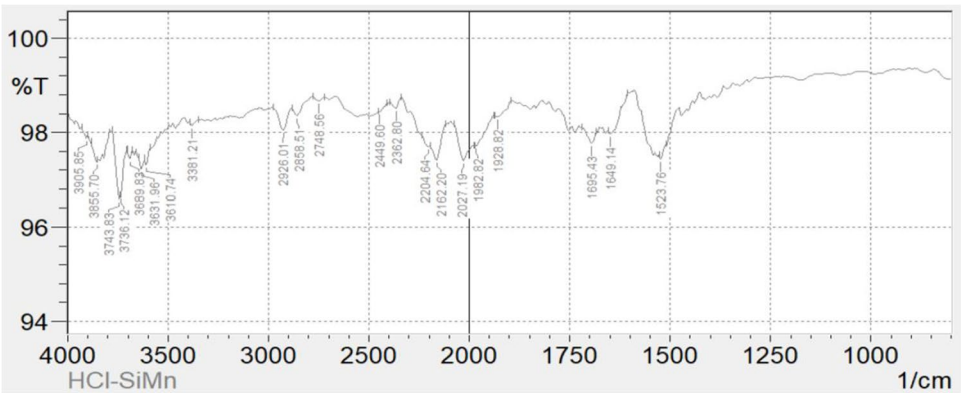

Fig. 16 FTIR spectrum graph for treated hydrochloric acid silicon manganese (HCl-SiMn)

silicon manganese slag [70–72]. In Fig. 15, the peak at 977 to 1176 cm^{-1} was due to asymmetric and symmetric tetrahedral of SiO or stretch vibration of Al_2O_3, whereas 977 cm^{-1} was due to vibration bending of Si-O-Si [71]. It also noted that H_2SO_4 had eliminated Na and Mg as shown by EDS/EDX and FTIR in Figs. 10, 17 and Table 8, which created the rough needle surface as shown in Fig. 3(d).

4 Conclusions

In conclusion, the compressive strength of silicon manganese concrete (SMC) achieved concrete strength of 37.3 MPa and 51.1 MPa at 28th day for the SMC30 and SMC50, respectively which complied with Grade 30 and Grade 50 standards. Alkali and acid modified the neat silicon manganese slag structure as shown by SEM, whereas the

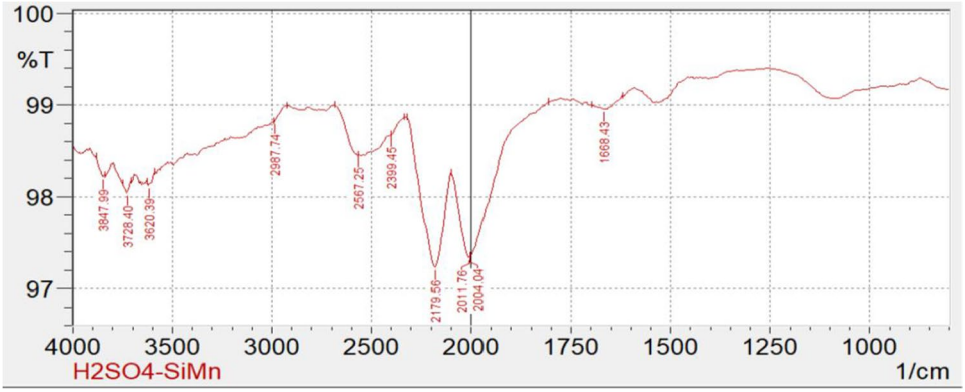

Fig. 17 FTIR spectrum graph for treated sulfuric acid silicon manganese (H_2SO_4-SiMn)

alkaline treatment smoothen the structure and acid treatment roughen the surface of the silicon manganese slag. FTIR showed there are significant change in the functional group which caused stretching and vibration of Si-O and Si-Mn functional groups of silicon manganese slag due to modifications, while EDS significantly showed the high content of both silicon (Si) and manganese (Mn) elements. Therefore, it was concluded that curing duration increases the strength of SMC, which is useful for fully replacement of NWC.

Acknowledgements The authors would like to thank and acknowledge Universiti Malaysia Sarawak (UNIMAS), Swinburne University of Technology Sarawak Campus, and OM Materials (Bintulu) Sdn. Bhd. for their support.

Authors' Contributions Chin Mei Yun and Muhammad Khusairy Bin Bakri fabricated and carried out the experiment with support from Perry Law Nyuk Khui. Chin Mei Yun and Muhammad Khusairy Bin Bakri wrote the manuscript. Md. Rezaur Rahman, Kuok King Kuok and Durul Huda check follow of writing and edit the technical part of the manuscript.

Data Availability Materials can be obtained from OM Materials Sdn. Bhd., Bintulu, Sarawak.

Declarations

Ethics Approval Not applicable.

Consent to Participate Not applicable.

Consent for Publication Not applicable.

Competing Interests The authors declare no competing interests.

References

1. Kim YJ, Jeon SJ, Choi MS, Kim YJ, Choi YW (2010) The quality properties of self consolidating concrete using lightweight aggregate. In: Oh BH, Choi OC, Chung L (eds.) Fracture Mechanics of Concrete and Concrete Structures – High Performance, Fiber Reinforced Concrete, Special Loadings and Structural Applications, pp. 1342–1346. https://framcos.org/FraMCoS-7/11-08.pdf
2. Lotfabadi P (2014) High-rise buildings and environmental factors. Renew Sust Energ Rev 38(1):285–295. https://doi.org/10.1016/j.rser.2014.05.024
3. Rossignolo JA, Agnesini MVC, Morais JA (2003) Properties of high-performance LWAC for precast structures with Brazilian lightweight aggregates. Cem Concr Compos 25(1):77–82. https://doi.org/10.1016/S0958-9465(01)00046-4
4. Chour H-B, Kim JM (2020) Properties of silicon manganese slag as an aggregate for concrete depending on cooling conditions. Journal of Material Cycle and Waste Management 22(1):1067–1080. https://doi.org/10.1007/s10163-020-01003-8
5. Yasar E, Atis CD, Kilic A, Gulsen H (2003) Strength properties of lightweight concrete made with basaltic pumice and Fly ash. Mater Lett 57(15):2267–2270. https://doi.org/10.1016/S0167-577X(03)00146-0
6. Oliveira RWH, Fernandes G, Sousa FC, Barreto RA (2017) Chemical and mineralogical characterization of silicon manganese Iron slag as railway ballast. REM International Engineering Journal 7(4):385–391. https://doi.org/10.1590/0370-44672017700019
7. Holm TA (1994) Lightweight concrete and aggregates. In: Klieger P, Lamond J (eds) Significance of tests and properties of concrete and concrete-making materials. ASTM International, pp 522–532. https://doi.org/10.1520/STP36447S
8. Manju K, Kumar BD, Kumar SS, Kumar SN (2018) Behaviour of concrete by using artificial aggregates A review. International Journal of Engineering & Technology 7(2.21):255–258. https://doi.org/10.14419/ijet.v7i2.21.12183
9. Frias M, de Rojas MIS, Santamaria J, Rodriquez C (2006) Recycling of silicomanganese slag as Pozzolanic material in Portland cements: basic and engineering properties. Cem Concr Res 36(3):487–491. https://doi.org/10.1016/j.cemconres.2005.06.014
10. Saxena S, Tembhurkar AR (2018) Impact of use of steel slag as coarse aggregate and wastewater on fresh and hardened properties of concrete. Construction and Building 165(1):126–137. https://doi.org/10.1016/j.conbuildmat.2018.01.030
11. Hainin MR, Yusoff NIM, Sabri MFM, Aziz MAA, Hameed MAS, Reshi WF (2012) (2012) steel slag as an aggregate replacement in Malaysian hot mix asphalt. ISRN Civil Engineering 1:1–5. https://doi.org/10.5402/2012/459016
12. Ismail S, How KW, Ramli M (2013) Sustainable aggregates: the potential and challenge for natural resources conservation. Procedia – social and behavioral. Science 101(1):100–109. https://doi.org/10.1016/j.sbspro.2013.07.183
13. Nor AM, Yahya Z, Abdullah MMAB, Razak RA, Ekaputri JJ, Faris MA, Hamzah HN (2016) A review on the manufacturing of lightweight aggregates using industrial by-product. MATEC

Web of Conferences 78(1):1–8. https://doi.org/10.1051/matecconf/20167801067
14. Sherly R, Kumar SS (2011) Valuable products from Fly ash - A review. J Ind Pollut Control 27(2):113–120 http://www.icontrolpollution.com/articles/valuable-products-from-fly-ash-a-review-1-4.pdf
15. Kumar S, Singh SK, Mishra SC (2018) Processing and characterization of Fly-ash compacts. Materials Today: Proceedings 5(2):3396–3402. https://doi.org/10.1016/j.matpr.2017.11.584
16. Hashmi AF, Haq MU (2018) Indian based fly ash & International Based fly ash: A review paper. IOP Conference Series: Materials Science and Engineering 404(1):1–5. https://doi.org/10.1088/1757-899X/404/1/012035
17. Ersoy B, Kavas T, Evcin A, Baspinar S, Sariisik A, Dikmen S (2009) Production of fired ceramic materials from Fly ash with Witherite additive. Afyon Kocatepe University Journal of Science and Engineering Sciences 9(3):45–52 https://dergipark.org.tr/tr/download/article-file/18735
18. Kim KD, Kang SG (2007) Manufacturing artificial lightweight aggregates using coal bottom ash and clay. Journal of Korean Crystal Growth and Crystal Technology 17(6):277–282 http://koreascience.kr/article/JAKO200706717302090.pdf
19. Ruthkowska G, Wichowski P, Franus M, Mendryk M, Fronczyk J (2020) Modification of ordinary concrete using Fly ash from combustion of municipal sewage sludge. Materials 13(2):487. https://doi.org/10.3390/ma13020487
20. Sun JS, Kim JM, Sung JH (2016) Evaluation on the applicability of dry processed bottom ash as lightweight aggregate for construction fields. Journal of Material Cycles and Waste Management 18(4):752–762. https://doi.org/10.1007/s10163-015-0367-x
21. Juenger MCG, Winnefeld F, Provis JL, Ideker JH (2011) Advances in alternative cementitious binders. Cem Concr Res 41(12):1232–1243. https://doi.org/10.1016/j.cemconres.2010.11.012
22. Ferronato N, Torretta V (2019) Waste mismanagement in developing countries: A review of global issues. Int J Environ Res Public Health 16(6):1060. https://doi.org/10.3390/ijerph16061060
23. Kambole C, Paige-Green P, Kupolati WK, Ndambuki JM, Adeboje A (2019) Comparison of technical and short-term environmental characteristics of weathered and fresh blast furnace slag aggregates for road base applications in South Africa. Case Studies in Construction Materials 11(1):1–13. https://doi.org/10.1016/j.cscm.2019.e00239
24. Neto JBF, Faria JOG, Fredericci C, Chotoli FF, Silva ANL, Ferraro BB, Ribeiro TR, Malynowskyj A, Q uarcioni, V.A., Lotto, A.A. (2015) Modification of molten steelmaking slag for cement application. Journal of Sustainable Metallurgy 2(1):13–27. https://doi.org/10.1007/s40831-015-0031-7
25. Yildrim IZ, Prezzi M (2011) (2011) chemical, mineralogical, and Morphological properties of steel slag. Advances in Civil Engineering 1:1–14. https://doi.org/10.1155/2011/463638
26. Wang H, Wang Y, Cui S, Wang J (2019) Reactivity and hydration property of synthetic air quenched slag with different chemical compositions. Materials 12(6):1–24. https://doi.org/10.3390/ma12060932
27. Altun IA, Yilmaz I (2002) Study on steel furnace slags with high MgO as additive in Portland cement. Cem Concr Res 32(8):1247–1249. https://doi.org/10.1016/S0008-8846(02)00763-9
28. Rojas MF, Rojas MIS (2004) Chemical assessment of the electric arc furnace slag as construction material: expansive compounds. Cem Concr Res 34(10):1881–1888. https://doi.org/10.1016/j.cemconres.2004.01.029
29. Kourounis S, Tsivilis S, Tsakiridis PE, Papadimitriou GD, Tsibouki Z (2007) Properties and hydration of blended cements with steelmaking slag. Cem Concr Res 37(6):815–822. https://doi.org/10.1016/j.cemconres.2007.03.008
30. Frias M, Rojas MIS, Santamaria J, Rodriguez C (2006) Recycling of silico-manganese slag as pozzolanic material in Portland cements: basic and engineering properties. Cem Concr Res 36(3):487–491. https://doi.org/10.1016/j.cemconres.2005.06.014
31. Choi S, Kim J, Oh S, Han D (2017) Hydro-thermal reaction according to the CaO/SiO2 mole-ratio in silico-manganese slag. Journal of Materials Cycles and Waste Management 19(1):374–381. https://doi.org/10.1007/s10163-015-0431-6
32. Patil AV, Pande AM (2011) Behaviour of silico manganese slag manufactured aggregate as material for road and rail track construction. Adv Mater Res 255(1):3258–3262. https://doi.org/10.4028/www.scientific.net/AMR.255-260.3258
33. Choi S, Kim J-M, Han D, Kim J-H (2016) Hydration properties of ladle furnace slag powder rapidly cooled by air. Constr Build Mater 113(1):682–690. https://doi.org/10.1016/j.conbuildmat.2016.03.089
34. ASTM C494-19 (2019) Standard specification for chemical admixtures for concrete. ASTM International, West Conshohocken. https://doi.org/10.1520/C0494_C0494M-19
35. BS 5075-1:1982 (1982) Concrete admixtures. Specification for accelerating admixtures, retarding admixtures and water reducing admixtures. British Standard
36. IS 10262:2019 (2019) Concrete Mix Proportioning — Guidelines. Indian Standard
37. ASTM E2015-04 (2014) Standard guide for preparation of plastics and polymeric specimens for microstructural examination. ASTM International, West Conshohocken. https://doi.org/10.1520/E2015-04R14
38. ASTM E2142-08 (2015) Standard test methods for rating and classifying inclusions in steel using the scanning Electron microscope. ASTM International, West Conshohocken. https://doi.org/10.1520/E2142-08R15
39. ASTM C1723-16 (2016) Standard guide for examination of hardened concrete using scanning Electron microscopy. ASTM International, West Conshohocken. https://doi.org/10.1520/C1723-16
40. ASTM E1508-12 (2019) Standard guide for quantitative analysis by energy-dispersive spectroscopy. ASTM International, West Conshohocken. https://doi.org/10.1520/E1508-12AR19
41. ASTM E168-16 (2016) Standard practices for general techniques of infrared quantitative analysis. ASTM International, West Conshohocken. https://doi.org/10.1520/E0168-16
42. ASTM E1252-98 (2013) Standard practice for general techniques for obtaining infrared spectra for qualitative analysis. ASTM International, West Conshohocken. https://doi.org/10.1520/E1252-98R13E01
43. BS EN 196-1:2016 (2016) Methods of testing cement. Determination of strength. British Standard
44. Ganesh G, Ramesh KV, Sudhakar C, Jagadeesh S (2017) Influence of silico manganese slag on mechanical and durability properties of concrete. International Journal of Civil Engineering and Technology (IJCIET) 9(7):1597–1604 http://www.iaeme.com/ijciet/issues.asp?JType=IJCIET&VType=9&IType=7
45. Balog A-A, Cobirzan N, Mosonyu E (2014) Microstructural analysis for investigation of limestone damages – A case study of the Fortress Wall of Cluj-Napoca. Romania Romanian Journal of Physics 59(5–6):608–613 http://www.nipne.ro/rjp/2014_59_5-6/0608_0613.pdf
46. Balog A-A, Cobirzan N, Barbu-Tudoran L (2014) Evaluation of limestone with non-invasive analytical methods. Romanian Journal of Physics 59(5–6):601–607 http://www.nipne.ro/rjp/2014_59_5-6/0601_0607.pdf
47. Johansson S, Sparrenbom C, Fiandaca G, Lindskog A, Olsson P-I, Dahlin T, Rosqvist H (2017). Geophys J Int 208(2):954–972. https://doi.org/10.1093/gji/ggw432

48. Mounia B, Merzoug B, Chaoki B, Djaouza AA (2013) Physico-chemical characterization of limestones and sandstones in a complex geological context, example north-East Constantine: preliminary results. IACSIT International Journal of Engineering and Technology 5(1):114–118 http://www.ijetch.org/papers/523-R029.pdf
49. Liu S, Yan P (2010) Effect of limestone powder on microstructure of concrete. Journal of Wuhan University of Technology – Materials Science Edition 25(1):328–331. https://doi.org/10.1007/s11595-010-2328-5
50. Chen JF, Sorelli L, Vandamme M, Ulm F-J, Chanvillard G (2010) A coupled Nanoindentation/SEM-EDS study on low water/cement ratio Portland cement paste: evidence for C–S–H/ca(OH)2 nanocomposites. J Am Ceram Soc 93(5):1484–1493. https://doi.org/10.1111/j.1551-2916.2009.03599.x
51. Awoyera PO, Olofinnade OM, Busari AA, Akinwumi II, Oyefesobi M, Ikemefuna M (2016) Performance of steel slag aggregate concrete with varied water-cement ratio. Jurnal Teknologi 78(10):125–131. https://doi.org/10.11113/jt.v78.8819
52. Anastasiou E, Papayianni I (2006) Criteria for the use of steel slag aggregates in concrete. In: Konsta-Gdoutos MS (ed) Measuring, monitoring and modeling concrete properties. Springer, Dordrecht. https://doi.org/10.1007/978-1-4020-5104-3_51
53. Oliveira RWH, Fernandes G, Sousa FC, Barreto RA (2017) Chemical and mineralogical characterization of silicon manganese iron slag as railway ballast. REM – international. Engineering Journal 70(4):385–391. https://doi.org/10.1590/0370-44672017700019
54. Akbar NA, Aziz HA, Adlan MN (2016) Potential of high quality limestone as adsorbent for Iron and manganese removal in groundwater. Jurnal Teknologi 78(9–4):77–82. https://doi.org/10.11113/jt.v78.9700
55. Awang H, Ahmad MH, Al-Mulali MZ (2015) Influence of Kenaf and polypropylene Fibres on mechanical and durability properties of fibre reinforced lightweight foamed concrete. Journal of Engineering Science and Technology 10(4):496–508 http://jestec.taylors.edu.my/Vol%2010%20issue%204%20April%202015/Volume%20(10)%20Issue%20(4)%20496-%20508.pdf
56. Lee S-T, Park D-W, Ann K-Y (2008) Mitigating effect of chloride ions on sulfate attack of cement mortars with or without silica fume. Can J Civ Eng 35(11):1210–1220. https://doi.org/10.1139/L08-065
57. Dawood ET, Ramli M (2012) Properties of high-strength Flowable mortar reinforced with palm fibers. International scholarly research notices. International Scholarly Research Notices 2012(1):1–5. https://doi.org/10.5402/2012/718549
58. Cao M, Ming X, He K, Li L, Shen S (2019) Effect of macro-, Micro- and Nano-calcium carbonate on properties of cementitious composites—A review. Materials 12(5):781. https://doi.org/10.3390/ma12050781
59. Kelestermur O, Yildiz S (2006) Effect of various NaCl concentration on corrosion of steel in concrete produced by addition of Styrofoam. Gazi University Journal of Science 19(3):163–172 https://dergipark.org.tr/tr/download/article-file/83098
60. Prucker F, Gjorv OE (2004) Effect of CaCl2 and NaCl additions on concrete corrosivity. Cem Concr Res 34(7):1209–1217. https://doi.org/10.1016/j.cemconres.2003.12.015
61. Quraishi MA, Nayak DK, Kumar D, Kumar V (2017) Corrosion of reinforced steel in concrete and its control: an overview. Journal of Steel Structures & Construction 3(1):1–6. https://doi.org/10.4172/2472-0437.1000
62. Bertolini L, Carsana M, Gastaldi M, Lollini F, Redaelli E (2016) Corrosion of Steel in Concrete and Its Prevention in Aggressive Chloride-Bearing Environments. 5th International Conference on Durability of Concrete Structures, 13–25. https://docs.lib.purdue.edu/cgi/viewcontent.cgi?article=1153&context=icdcs
63. Steenkamp JD, Maphutha P, Makwarela O, Banda WK, Thobadi I, Sitefane M, Gous J, Sutherland JJ (2018) Silicomanganese production at Transalloys in the twenty-tens. J South Afr Inst Min Metall 118(3):309–320. https://doi.org/10.17159/2411-9717/2018/v118n3a13
64. Jagadeesh S, Ramesh KV, Ganesh S, Kumar DSS (2018) Study on tensile strength properties of recycled aggregate concrete with and without Pozzolanic materials. International Journal of Civil Engineering and Technology (IJCIET) 9(11):671–679 http://www.iaeme.com/ijciet/issues.asp?JType=IJCIET&VType=9&IType=11
65. Ringdalen E, Gaal S, Tangstad M, Ostrovski O (2010) Ore melting and reduction in silicomanganese production. Metall Mater Trans B 41(1):1220–1229. https://doi.org/10.1007/s11663-010-9350-z
66. Al-Degs YS, El-Barghouthi MI, Issa AA, Khraisheh MA, Walker GM (2006) Sorption of Zn(II), Pb(II), and co(II) using natural sorbents: equilibrium and kinetic studies. Water Res 40(14):2645. https://doi.org/10.1016/j.watres.2006.05.018
67. Preeti SN, Singh BK (2007) Instrumental characterization of clay by XRF, XRD and FTIR. Bull Mater Sci 30(1):235–238. https://doi.org/10.1007/s12034-007-0042-5
68. Gunasekaran S, Anbalagan G (2007) Spectroscopic characterization of natural calcite minerals. Spectrochim Acta A Mol Biomol Spectrosc 68(3):656–664. https://doi.org/10.1016/j.saa.2006.12.043
69. Hajjaji M, Kacim S, Alami A, El Bouadili A, El Mountassir M (2001) Chemical and mineralogical characterization of a clay taken from the Moroccan Meseta and a study of the interaction between its fine fraction and methylene blue. Appl Clay Sci 20(1–2):1–12. https://doi.org/10.1016/S0169-1317(00)00041-7
70. Wang YG, Han F-I, Zhao S-Z, Mym H-Q (2017) Preparation and characterization of manganese slag and Fly ash-based Geopolymer. MATEC Web of Conferences 130(1):1–4. https://doi.org/10.1051/matecconf/201713004006
71. Xing X, Pang Z, Zheng J, Du Y, Ren S, Ju J (2020) Effect of MgO and K_2O on high-Al silicon-manganese alloy slag viscosity and structure. Minerals 10(9):810. https://doi.org/10.3390/min10090810
72. Andres ES, Prado AD, Martinez FL, Martil I (2000) Rapid thermal annealing effects on the structural properties and density of defects in SiO2 and SiNx:H films deposited by electron cyclotron resonance. J Appl Phys 87(1187):1–10. https://doi.org/10.1063/1.371996